Hindawi
Geofluids
Volume 2023, Article ID 3792978, 14 pages
https://doi.org/10.1155/2023/3792978

Research Article

Numerical Study on Deformation and Failure Characteristics of Rectangular Roadway

Xuejia Li,[1,2] Baoyang Wu,[1] Yanzhao Zhu,[3,4] Junting Guo,[1,3] and Zhaolong Li[3]

[1]*State Key Laboratory of Water Resource Protection and Utilization in Coal Mining, Beijing 102209, China*
[2]*National Energy Shendong Coal Technology Research Institute, Yulin 719000, China*
[3]*School of Energy and Mining Engineering, China University of Mining and Technology (Beijing), Beijing 100083, China*
[4]*State Key Laboratory Cultivation Base for Gas Geology and Gas Control (Henan Polytechnic University), Jiaozuo 454003, China*

Correspondence should be addressed to Yanzhao Zhu; zyzzgkd@163.com

Received 16 August 2022; Revised 4 November 2022; Accepted 24 November 2022; Published 20 January 2023

Academic Editor: Yi Xue

In the practical processes of coal mines and tunnel, rectangular roadways are widely used in the underground environment. However, the stress distribution law of the rock mass around the rectangular roadways is relatively complicated that is influenced by different parameters, such as the in situ stress, geological structure, and properties of the surrounding rock mass. It is extremely significant to conduct systematic and in-depth research regarding the stress distribution and deformation failure mechanism of the rock mass around the rectangular roadways. Based on theoretical analysis, the stress distribution law of the surrounding rock of rectangular roadway under different rock mass strength grades is studied directly through rectangular roadway in this paper. This further reveals the distribution law of secondary stress field after excavation of rectangular roadway. A coal mine intends to excavate a roadway in rock mass, and then, the rectangular roadway is simulated by FLAC3D software. Then, the strain distribution and failure types of roadway surrounding rock under different rock mass properties are obtained. The results show that the failure of rectangular roadway is mainly shear failure and tensile failure. The roof and floor of roadway are mainly tensile failure, and the side of roadway is mainly shear failure. Moreover, the stress shifting and distribution of the rock mass around rectangular roadways is a complicated dynamic variation process. The damage degree of the floor and roof of the rectangular roadway is greater than that of the two sides of the roadway. Its variation is mainly related to the strength of surrounding rock mass.

1. Introduction

With the development of economy, the demand for coal is also increasing day by day, and the mining of coal in China is gradually extended to deep underground rock strata, and the complexity of geological conditions increases accordingly. Moreover, the quantity of roadways in rock mass increases continuously. The stability issues of roadways become an important research topic [1–3]. Before the coal resources were excavated, the original in situ stress mode remains. However, the exploiting of coal mines changes the original in situ stress field and displacement field. Consequently, the previous stress equilibrium situation is influenced. The balance of the original stress field is broken, which will lead to the redistribution of stress, and this leads to the new stress distribution in the rock mass. In the stress concentration area, high stress leads to the deformation failure of the roadways in coal mines [4, 5]. The variation of those stresses results in the generation of the new stress field around the mining area. The redistribution of stress and the rebalance of rock structure will lead to some new failures. As a consequence, research on the distribution field of the stress and displacement in the surrounding rock mass plays a significant role in guaranteeing the safe mining of coal mines.

Safe mining of coal has always been the top priority of coal mining, and rock tunnel support and reinforcement is also an important research topic of coal mine safety production [6, 7]. Scholars have different research results in this regard. Shan et al., based on theoretical analysis and numerical simulation, concluded that the corner of roadway is the

core area of roadway support, and strengthening its support strength is conducive to improving the overall stability of roadway [8]. In addition, Chen et al. studied the influence of bolt support on the stability of reinforced rock mass and carried out theoretical analysis [9].

For the stress state of surrounding rock of roadway, most scholars adopt equivalent circle method. However, for rectangular roadway, the equivalent circle method can not well explain the failure of some rectangular roadway, nor can it get the stress distribution on both sides, top, and bottom of rectangular roadway. As shown in Figure 1, the stress distribution law in the surrounding rock mass of rectangular roadways is plotted [10].

Under the influence of the in situ stress, relative larger compressive stress occurs in the rock mass that is around the rectangular roadway side. In the horizontal direction, the principal tangential stress on both sides of the roadway first increases and then decreases to the original rock stress with the increase of the distance from the roadway center. The tensile tangential stress state is at the top of the rectangular roadway and reaches the maximum in the middle of the roadway top. As the distance from the rectangular roadway increases, the tensile stress gradually decreases and becomes compressive stress and then increases to the original rock stress. However, as for the radial compressive stress, it increases from zero to the original in situ stress. At the top corner of the roadway, the stress concentration is obvious, and the size of the stress is affected by the curvature radius. When the curvature radius is large, the stress concentration is inversely small. Around the corner, the stress concentration coefficient ranges from 2 to 5.

It is more significant to study the stress and strain state of surrounding rock directly through the angle of rectangular roadway. This paper adopted the numerical software of FLAC3D. The numerical analysis regarding the roadway stability was designed and performed. Moreover, valuable and beneficial conclusions were drawn.

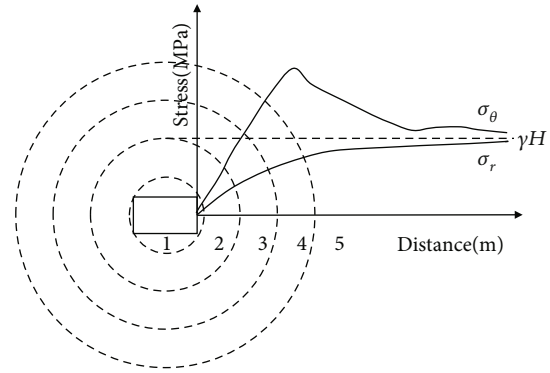

1-damaged zone, 2-fractured zone, 3-plastic zone, 4-elastic zone, 5-original in-situ stress zone, σ_θ-tangential stress, σ_r-radial stress, γ-volume weight of rock strata, H-buried depth

Figure 1: Stress distribution of the roadway periphery based on the equivalent circle analysis. 1: damaged zone; 2: fractured zone; 3: plastic zone; 4: elastic zone; 5: original in situ stress zone; σ_θ: tangential stress; σ_r: radial stress; γ: volume weight of rock strata; H: buried depth.

2. Numerical Model and Determination of Parameters

2.1. Establishment of the Numerical Model. A coal mine in China plans to dig a large cross-sectional roadway into rock formations. The cross-sectional geometry of the road is rectangular. For the cross section of this road, the width is 8 m, and the wall height is 8 m. Its main mechanical parameters are listed in Table 1. The numerical software FLAC3D was used for this simulation. The actual geometric size of the road is 80 m × 100 m × 90 m. The self-weight of the overlying rock mass of the rectangular tunnel is taken as the vertical stress of the top surface of the numerical model, the vertical displacement of the bottom surface of the numerical model is fixed to zero, and the horizontal displacement of the left and right sides of the horizontal numerical model is fixed to zero. To simulate this geometry, the parallel hexahedral radial mesh was used. Specifically, it is totally composed of 16400 zones and 17602 grid points. The Mohr-Coulomb constitutive model is used for numerical simulation, as shown in Figure 1. At the center of this numerical model, it is a roadway embedded in the rock strata. The cross-sectional plane at $Y = 20$ was selected. Moreover, being parallel with the positive axis x, five measuring points with the equal distance were arranged, namely, the point 1, point 2, point 3, point 4, and point 5. The distance between the point 1 and the rock roadway side is 0.5 m. In addition, parallel to the positive axis x, five equidistant measuring points are arranged, namely, points 1, 2, 3, 4, and 5. The distance between point 1 and the rock roadway side is 0.5 m. The distance between the remaining measurement points and the previous measurement point is 2.5 m, and five measurement points are arranged, namely, points A, B, C, D, and E. The distance between measuring point A and rock roadway roof is 1 m. Along the positive direction of z-axis, the distance between measuring point A and the previous measuring point is 2.5 m, as shown in Figure 2.

2.2. Determination of Parameters. The numerical model mainly consists of three different types of rock formations, namely, mudstone, fine sandstone, siltstone, and coal. The geometric dimensions of the road are 8 m in width and 8 m in height. The roadway is excavated in the mudstone layer, which is at the bottom of the coal seam. The practical in situ observation shows that the principal stresses are 16.2 MPa, 12.6 MPa, and 7.5 MPa. The main mechanical parameters of each rock stratum are obtained by sampling and mechanical test. The primary mechanical parameters of the rock strata are tabulated in Table 1. Carry out parameter analysis to further determine the distribution law of stress and strain under the influence of various parameters. In addition to those, the range of the plastic area is studied.

3. Validation of This Numerical Model and Result Analysis

3.1. Validation of This Numerical Model. To validate the credibility of this numerical model, preliminary running was conducted on it. Then, the distributions of the

Table 1: Mechanical parameters of the principal rock strata.

Rock	Bulk modulus E (GPa)	Shear modulus G (GPa)	Poisson's ratio ν	Volume weight (t/m^3)	Internal friction angle φ (°)
Mudstone	19.3	32.3	0.38	2.6	27.8
Fine sandstone	26.3	43	0.22	2.65	32.1
Siltstone	20	56.3	0.26	2.65	35
Coal	6	10.9	0.35	1.4	16

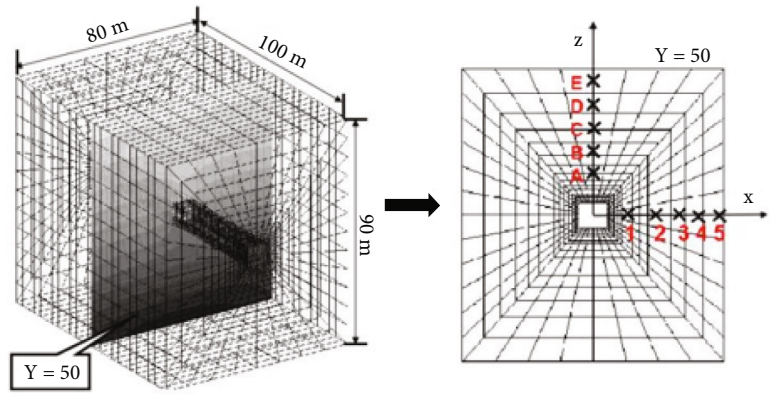

Figure 2: Numerical calculation model and the schematic diagram showing the measuring point location.

maximum stress and minimum stress were acquired. The results show that there is a close match between the acquired result and the stress distribution around the rectangular roadway which was indicated in the reference book of "Mine Pressure and Strata Control" by Minggao Qian [10]. More specifically, the numerical simulation result is shown in Figure 3.

According to the numerical simulation results, there is a tensile stress zone in the middle of the rectangular roadway roof. When the tensile strength limit of roadway surrounding rock is reached, the roadway roof surrounding rock will be subject to tensile failure. There is a large compressive stress on both sides of the roadway, which reaches the maximum in the middle of the edge of the roadway, and the further away from the roadway, the lower the initial in situ stress gradually. Specifically, it can be summarized as follows: (1) in the center of roadway roof and floor, tensile stress area appears, as shown in the dashed line in Figure 3. The tensile stress is the largest around the boundary near the roadway. In the deep rock mass around the roadway, the stress is mainly transferred from tensile stress to compressive stress. Then, it shifts to the original in situ stress state; (2) relatively large compressive stress will appear on both sides of rectangular roadway. In the middle of the periphery, it is the largest. In the deep region, it gradually decreases to the original in situ stress; (3) shear stress is concentrated at the corner of rectangular roadway. The greater the curvature, the more concentrated the stress.

3.2. Research on the Stress Distribution Law in the Surrounding Rock Mass around the Roadway. After the roadway was excavated, the stress contour is shown in Figure 4. The principal stress on the surface of both sides of the rectangular roadway is the minimum. With the increase of the distance between the side and the inner section of the roadway, the principal stress reaches the maximum and then decreases gradually. At the middle of the roadway roof and the roadway floor, the tensile stress concentration occurs [11, 12]. Based on this figure, it can be known that in the surrounding rock mass around the roadway, the four corner shear stresses around the cross section of rectangular roadway reach the maximum, and obvious stress concentration occurs.

Based on Figure 4(a), it can be known that for the floor that has the strength level like this, the tensile stress is concentrated at the top of the rectangular roadway under the influence of vertical stress and relatively high horizontal stress. When the external tensile stress reaches or even exceeds the critical strength of the roof strata, tensile failure gradually occurs from the bottom to the top of the roof. Under the influence of the support pressure in the rectangular roadway roof, the two sides of the rectangular roadway moved to the inner section of the roadway, so that the roadway roof sank and deformed. When the rock stratum strength of the roadway floor is large, the roadway floor may bend and deform upward under the combined influence of the support pressure and horizontal in situ stress on both sides of the roadway. However, when the rock stratum strength of the roadway floor is low, the roadway floor will be damaged by tensile cracks from top to bottom, resulting in serious floor heave disaster.

Based on Figure 4(b), it can be known that the stress in the surrounding rock will be redistributed after road excavation. Large support pressure appears on both sides of the roadway. When the strength of rock mass on both sides of the roadway is weak, under the influence of support pressure and horizontal tectonic stress, elastic-plastic deformation occurs, and when it reaches equilibrium, a critical

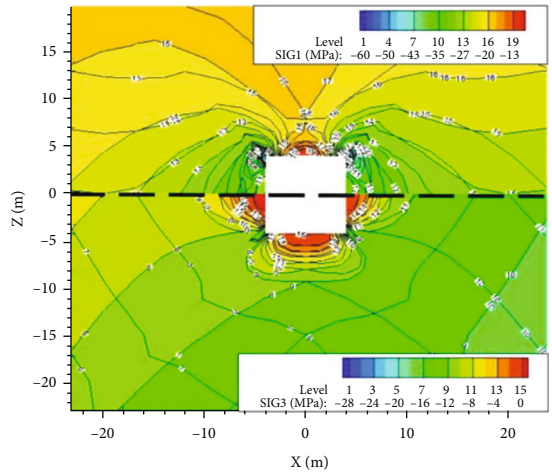

(a) Numerical result about the stress distribution around the roadway periphery

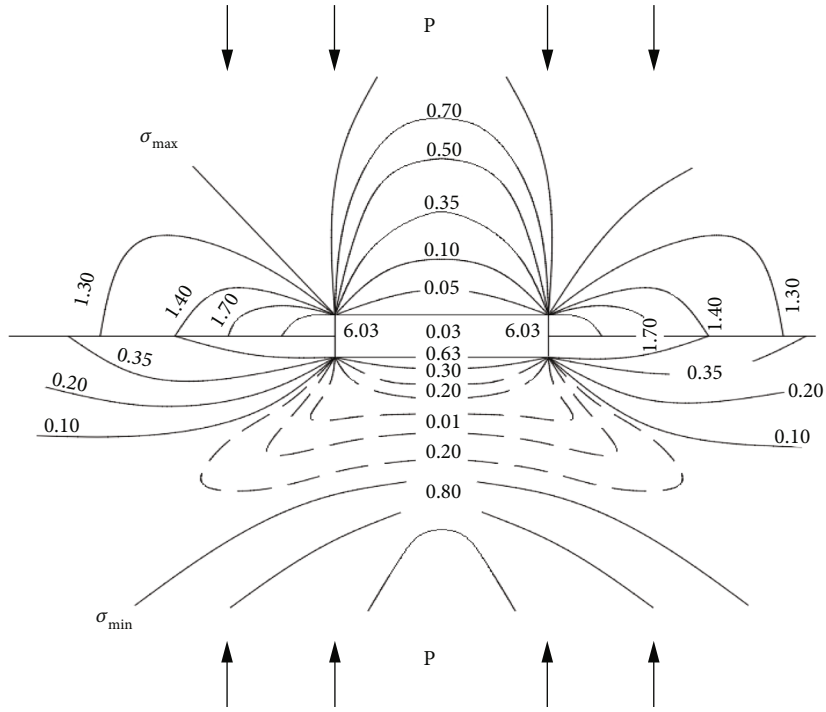

(b) Stress distribution around the periphery of the rectangular roadway

Figure 3: Validation of the numerical model.

equilibrium zone and an elastic zone are formed. Tensile failure occurs on the surface of surrounding rock mass.

It can be seen from Figures 4(a) and 4(b) that tangential compression stress is the main part of roof stress after rectangular roadway excavation. Through the comparison of these two figures, it is found that the vertical stress is higher than the horizontal stress.

Figure 5 shows the results of the cross section of the rectangular roadway at position $Y = 50$. The horizontal axis represents the distance between the measuring points arranged in the rock mass and the center point of the rectangular roadway (point O). The vertical axis shows the stress value at the measurement point. Figure 5(a) shows that at the initial stage, with the increase of the center distance from the rectangular roadway, the stress increases gradually, and at the later stage, the stress increases gently. Figure 5(a) shows that, in the vertical direction, the stress increases gradually with the increase of the center distance from the rectangular roadway in the initial stage, and the stress increases gently in the later stage. Figure 5(b) shows that, in the horizontal direction, with the increase of the distance from the center point of the rectangular tunnel, the stress increases first and then decreases gradually. At two sides of the roadway, unequal stress distribution occurs.

3.3. Research on the Displacement Distribution Law in the Surrounding Rock Mass around the Roadway. After the rectangular roadway is excavated, in the surrounding shallow

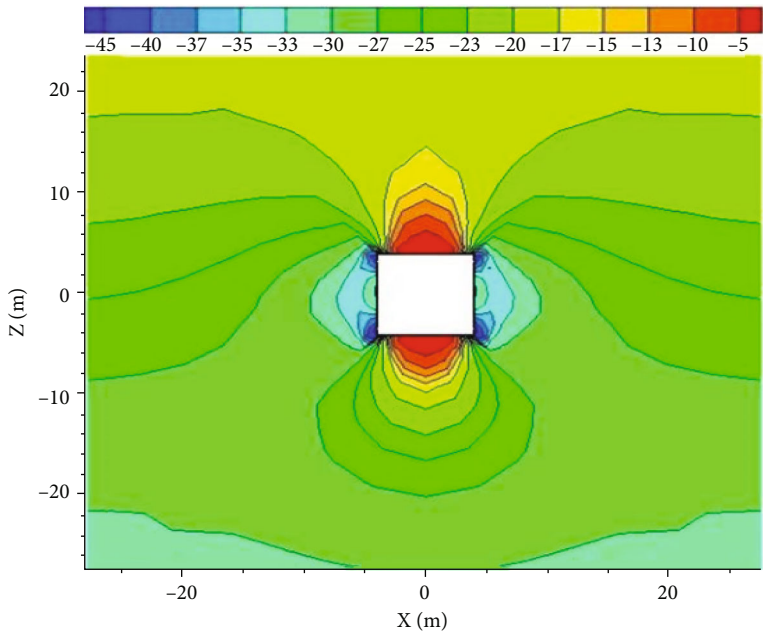

(a) Contour of the stress distribution along the Z direction

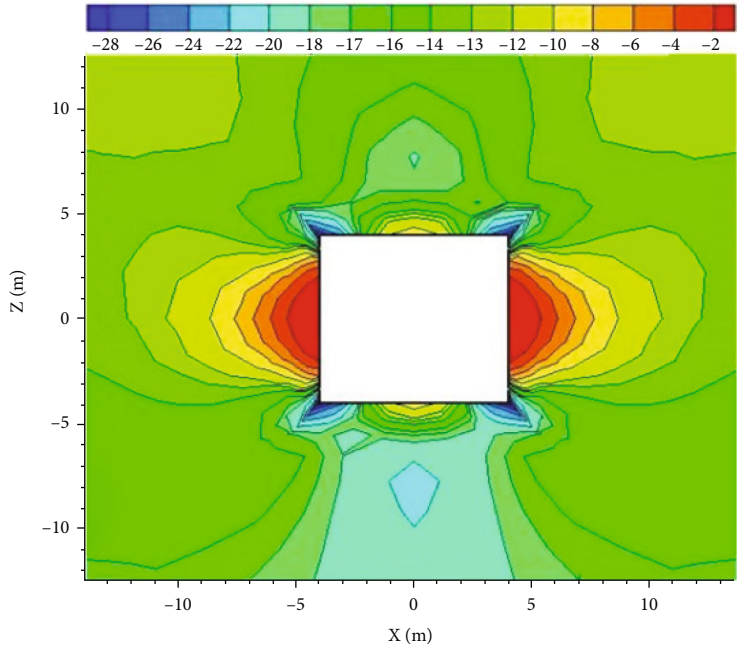

(b) Contour of the stress distribution along the X direction

Figure 4: Contour of the stress distribution.

rock mass of the roadway, plastic zone has relatively large area generates. Tensile failure occurs in the central area of the roadway floor and roof. In the vertical direction, shear failure occurs with the increase of the distance from the roadway. In the horizontal direction, large area shear failure will occur on both sides of the roadway. At the corner of rectangular roadway, the depth of plastic zone is relatively large. This indicates that the surrounding rock is seriously damaged in this area.

According to Figure 6(b), it can be seen that the stress in surrounding rock is redistributed after rectangular excavation. In addition, on both sides of the roadway, relatively large support pressure will be generated. When the strength of rock mass on both sides of roadway is relatively low, elastic-plastic deformation occurs under the influence of support pressure and horizontal tectonic stress. Then, the critical equilibrium region and the elastic region are formed. On the surface of surrounding rock, tensile crack failure occurs, and uplift is generated inside the rectangular roadway.

Based on Figure 7, it can be known that along the direction of axis x, both sides of the rectangular roadway move to the central part under the influence of horizontal stress.

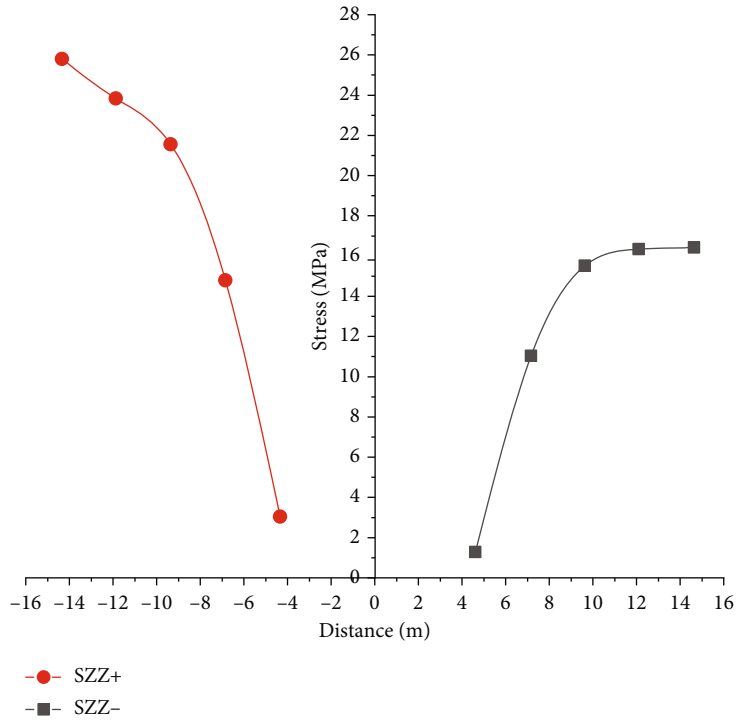

(a) The final stress distribution along the direction of Z

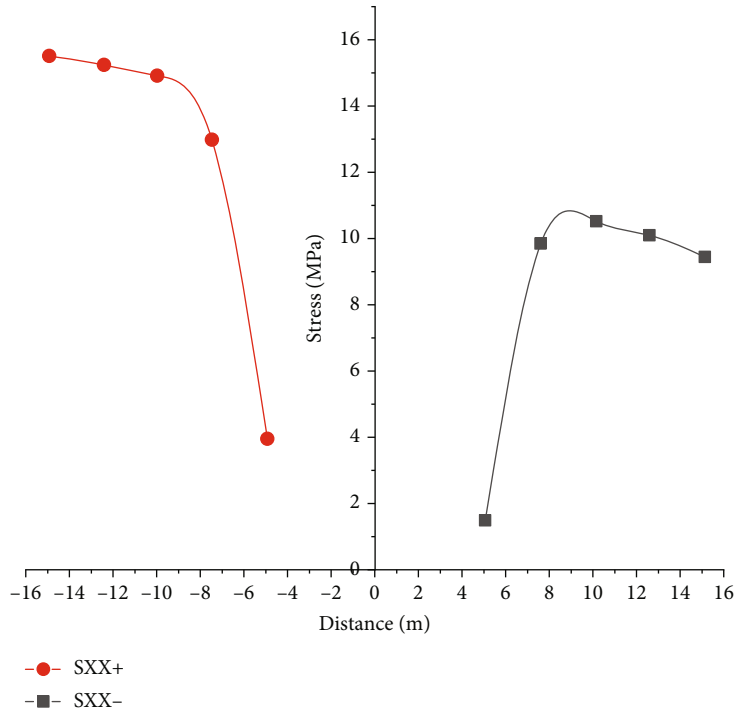

(b) The final stress distribution along the direction of X

Figure 5: The equilibrium stress distribution after the roadway is excavated.

However, the change is not so obvious. In the horizontal direction, with the increase of the distance from the roadway, the rock mass is at a stage that is not affected by the surrounding rock stress of the roadway. Even if the displacement deviates from the road centerline, the displacement value is relatively small and can be ignored. According to Figure 7(a), along the z-axis direction, the roadway roof is affected by vertical stress and has a displacement of 48 mm. At the same time, the roadway floor has a floor heave, and the floor heave displacement is 30 mm. As a consequence, there is a gradual increasing impact, and there is a gradual increasing trend. In the roadway floor, with the distance to

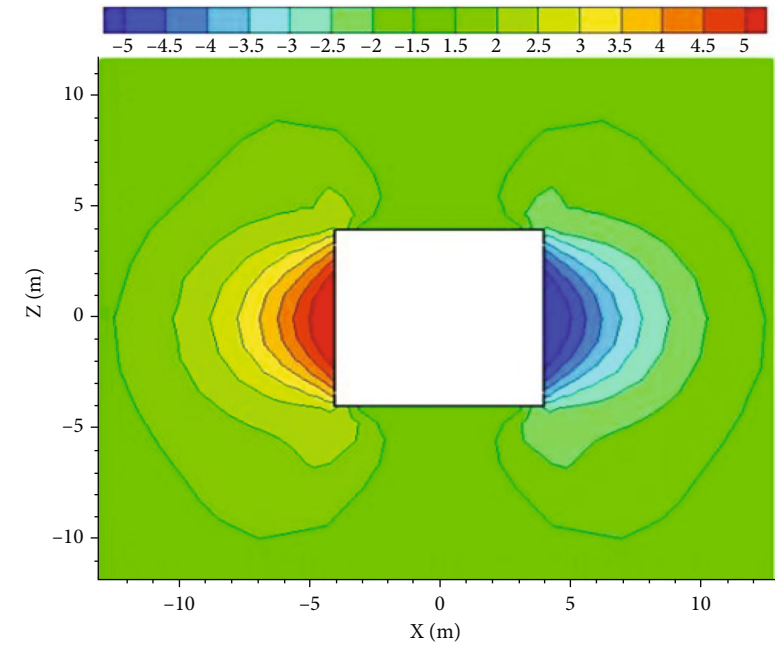

(a) Displacement along the direction of Z

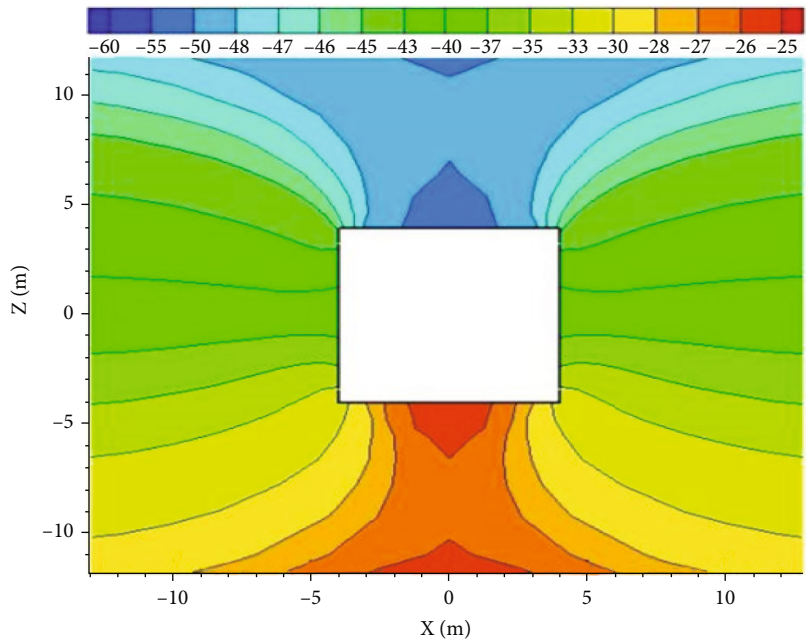

(b) Displacement along the direction of X

Figure 6: Contour of the displacement for the roadway.

the roadway further increasing, the disturbing that is suffered is smaller. As a consequence, with the distance to the roadway further increasing, the deformation of the surrounding rock mass becomes smaller.

4. Parameter Analysis

In kinds of numerical simulation methods, the finite difference method is widely used. Among them, the most widely used software is the FLAC3D which is designed based on the fast Lagrangian analysis method. The operation of this program is simple, and the application is wide [13]. Moreover, it can be used in the tunnelling engineering, landslide, and foundation trench. And it is especially suitable for the rock and soil engineering [14–17]. In addition to those, in this program, the structural element is incorporated, such as the cable element and the pile element. Those structural elements can be used to simulate the rock reinforcement tendons, such as the rock bolt and cable bolt. And those structural elements can be modified by the users to realise the special purposes [18, 19]. For the research on the stability of the rock mass around the roadway [20], the most

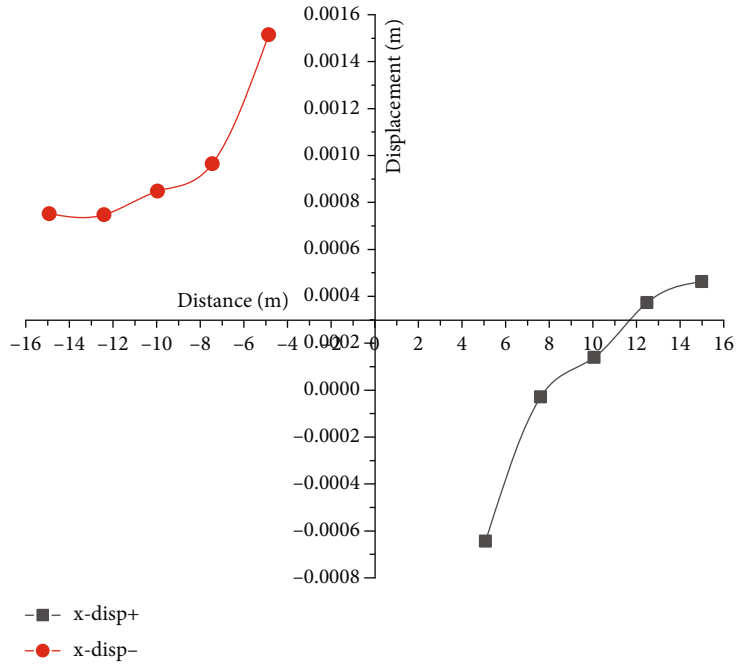

(a) Displacement along the direction of X

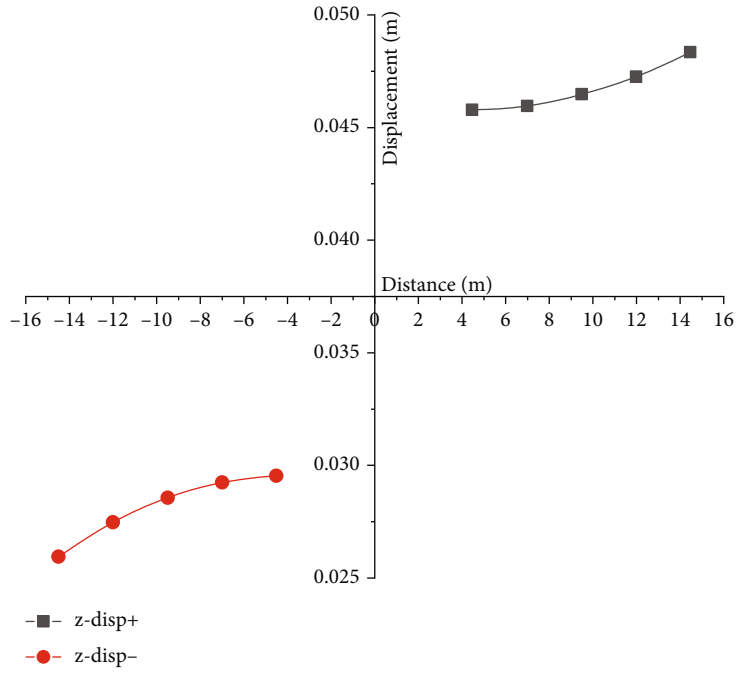

(b) Displacement along the direction of Z

Figure 7: Displacement curve of the roadway.

widely used constitutive law is the Mohr-Coulomb model. The project has different geological conditions, so it is important to set reasonable parameters when using the FLAC3D software to simulate the tunnel. In the numerical calculation, how to select the appropriate parameters for the constitutive model to guarantee the rationality of the calculated results is a valuable research topic.

Figures 8 and 9 show the distribution of plastic zone after excavation of rectangular roadway. When rectangular roadway is excavated, the stress is redistributed in the surrounding rock of rectangular roadway. This will lead to yield failure of surrounding rock. According to the existing research, the study of the volume or range of plastic zone is closely related to the size of surrounding rock stress and geotechnical properties, which is of great significance to the stability of surrounding rock. When analysing the stability of the surrounding rock mass, the influence of the plastic zone cannot be

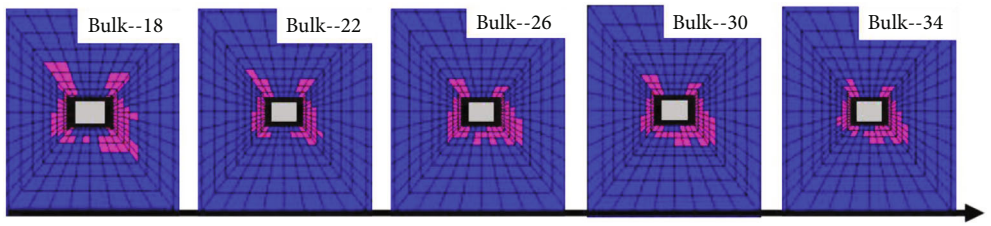

Figure 8: Variation of the plastic zone when the bulk modulus changes.

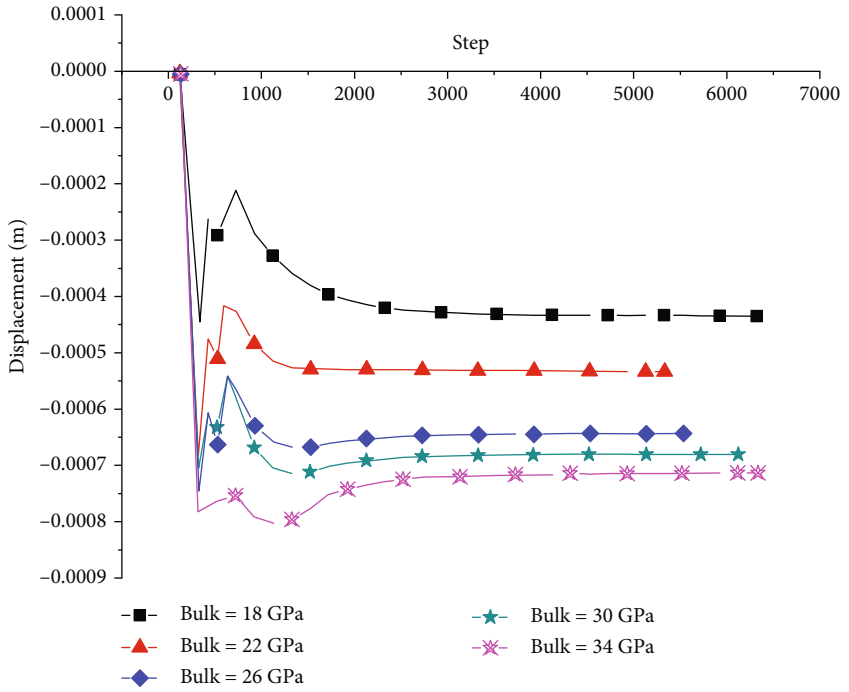

(a) Displacement along the horizontal direction

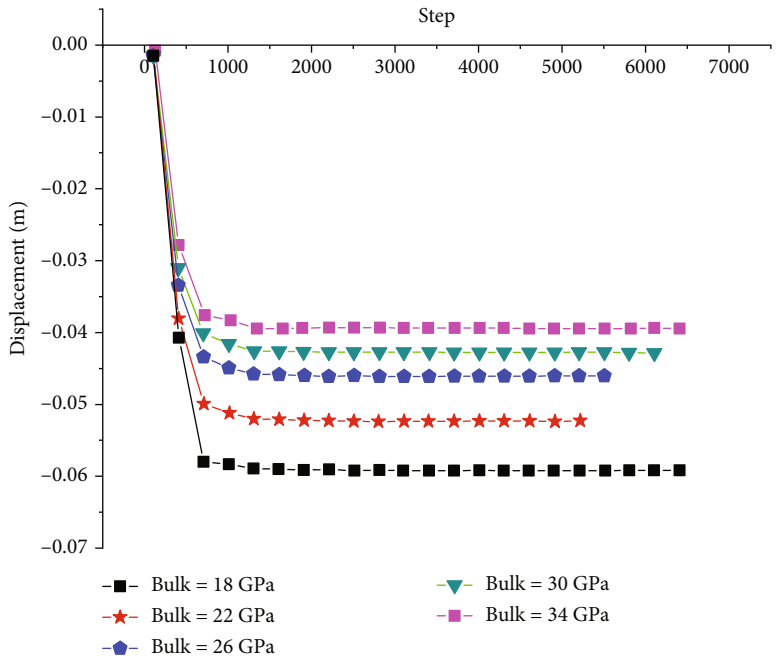

(b) Displacement along the vertical direction

Figure 9: Displacement magnitude under the condition that the bulk modulus changes.

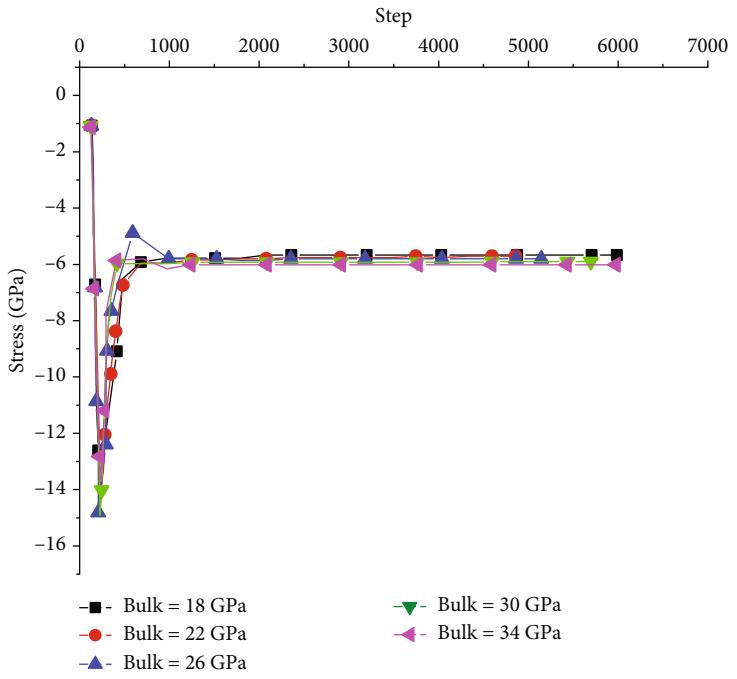

(a) Stress along the horizontal direction

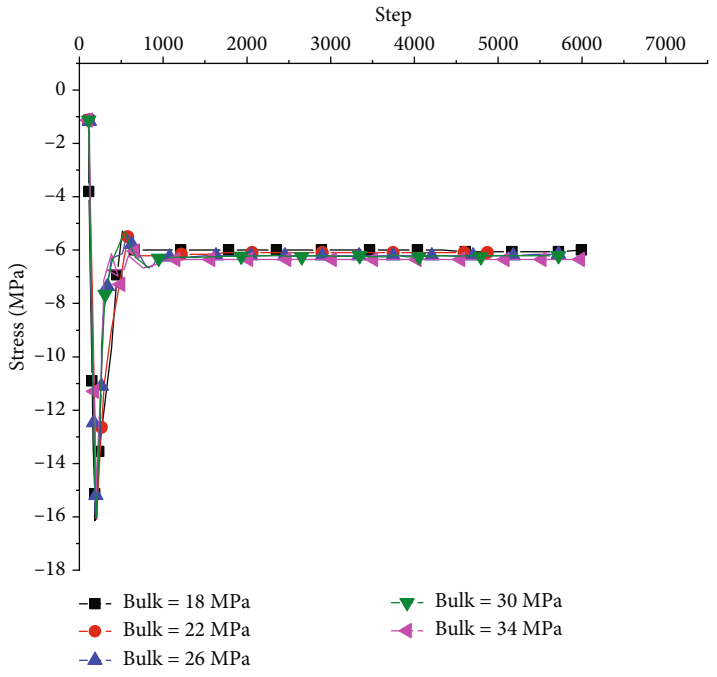

(b) Stress along the vertical direction

Figure 10: Variation of the stress under the condition that the bulk modulus changes.

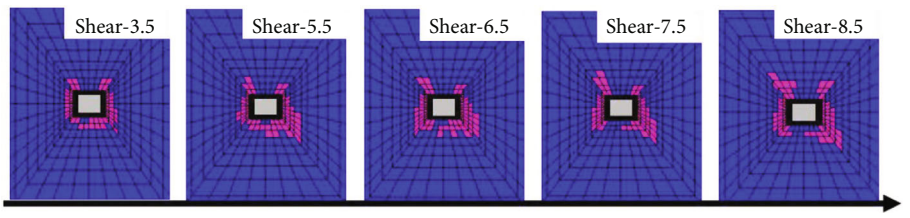

Figure 11: Plastic deformation of the rock mass around the roadway when the shear modulus is different.

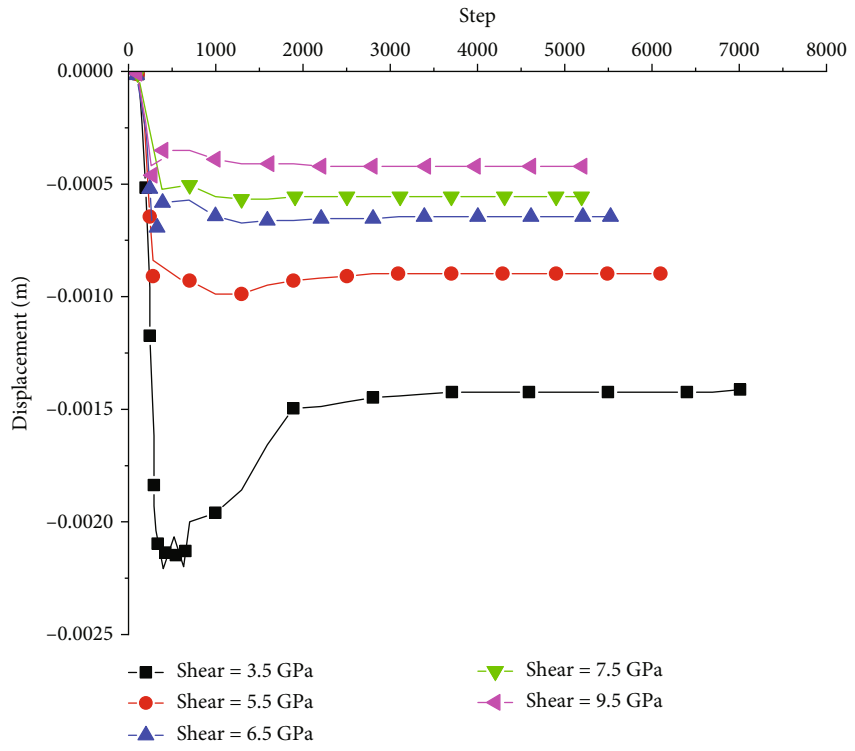

(a) Displacement along the direction of x-axis

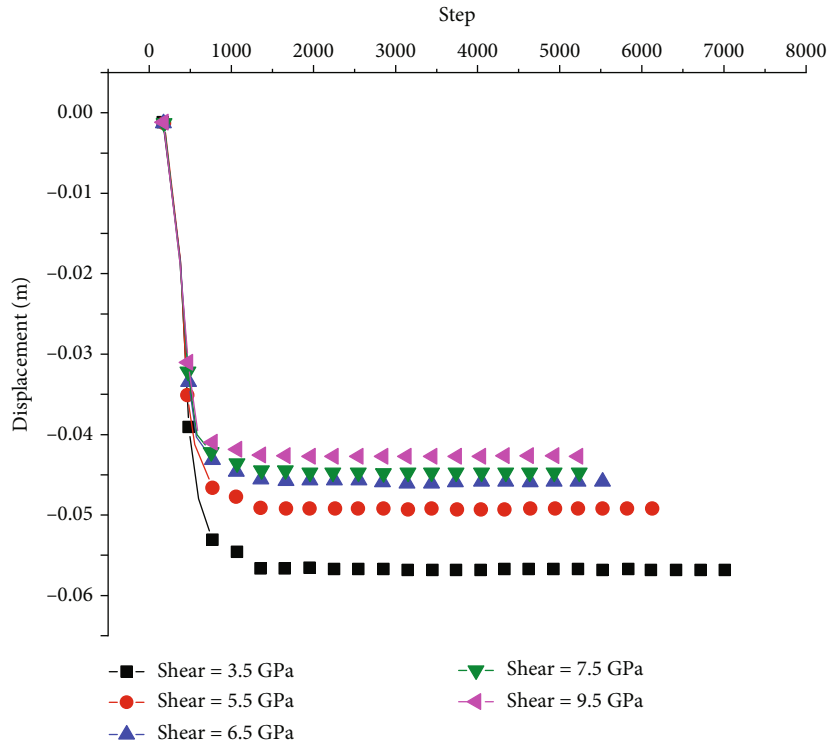

(b) Displacement along the direction of y-axis

Figure 12: Displacement magnitude under the condition that the shear modulus is different.

neglected. Based on Figure 8, it can be known that the range of the plastic zone in the roadway side is larger than the range of the plastic zone in the roof. This indicates that when the roadway is excavated, instability issues are likely to occur in the roadway sides. This place should be the core position in the roadway support. During the construction process, special emphasis should be given to this section.

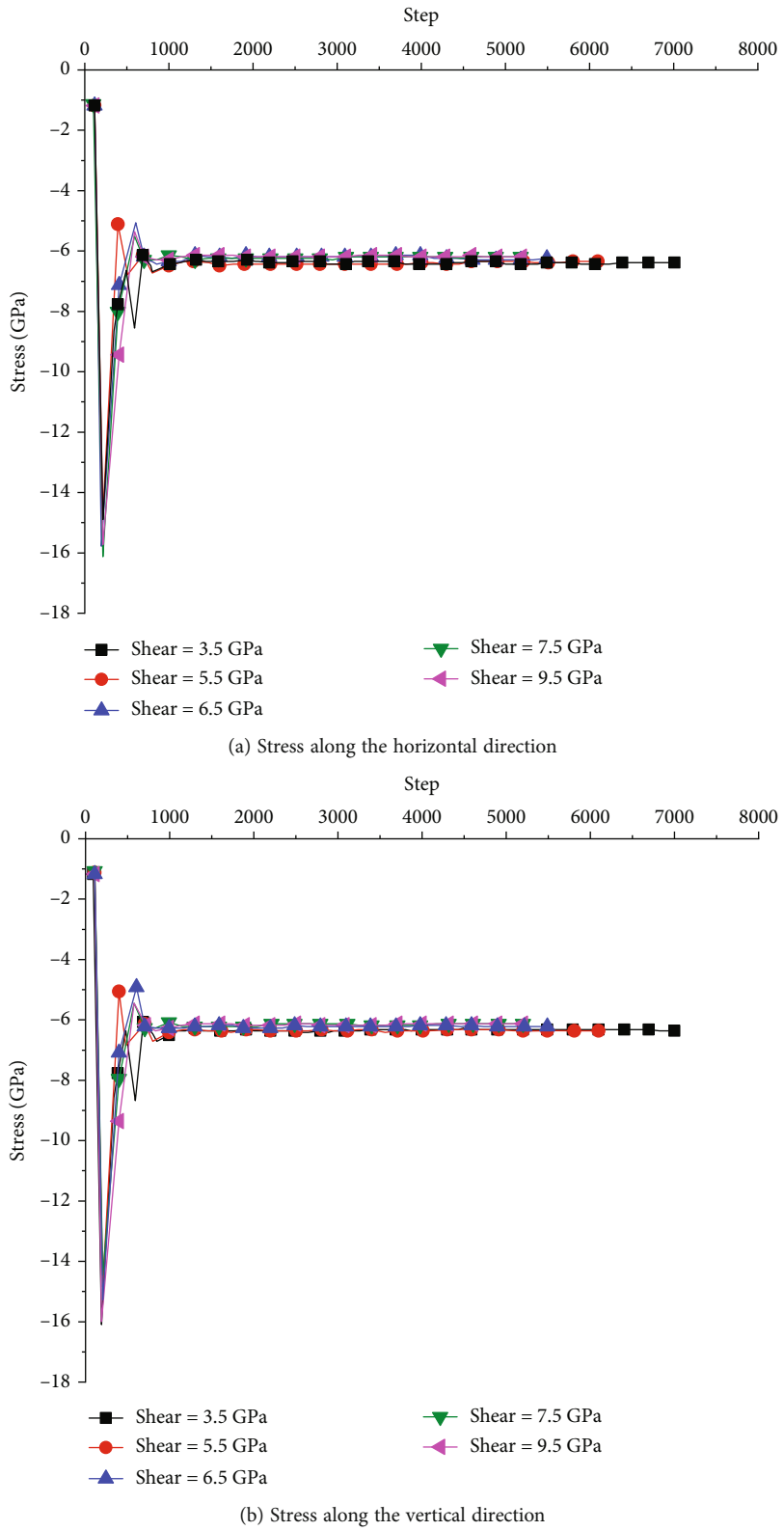

(a) Stress along the horizontal direction

(b) Stress along the vertical direction

Figure 13: Variation of the stress when the shear modulus is different.

4.1. Bulk Modulus. Figure 8 shows the variation of the plastic zone when the bulk modulus changes. Based on this figure, it can be known that when the bulk modulus of the surrounding rock mass around the roadway increases, the distribution of the plastic zone shifts from those four corners of the roadway to the periphery of the roadway. Moreover, at the

corners, the shear failure declines. Then, the stress in the roadway floor increases, and this will lead to the generation of the tensile failure.

Figure 9 shows the displacement magnitude under the condition that the bulk modulus changes. Initially, with the increase of the bulk modulus, the displacement of the surrounding rock mass along the X direction gradually increases. When the bulk modulus continues to increase, the increase of the deformation of the surrounding rock mass decreases. Furthermore, with the increase of bulk modulus, the influence on tunnel deformation decreases. The displacement along the z-axis will decrease as the bulk modulus increases. This shows that when the surrounding rock has a large strength, it can produce favorable supporting effects.

Figure 10 shows the stress at the measuring point 1# when the bulk modulus is different. The figure shows that the change of bulk modulus has no obvious influence on the stress distribution in the surrounding rock around the roadway. As a whole, with the increase of bulk modulus, the stress of surrounding rock of roadway increases, but the amplitude of stress increase is small.

4.2. Shear Modulus. Figure 11 shows the plastic deformation when the shear modulus is different. According to the figure, the change of shear modulus has a significant impact on the stress distribution of surrounding rock around the roadway. The plastic zone at the corner of the rectangular tunnel has a large range and volume, which indicates that the damage at the corner is relatively serious. According to the figure, the change of shear modulus has a significant impact on the stress distribution of surrounding rock around the roadway. The plastic zone at the upper corner of the rectangular tunnel has a large range and volume, which indicates that the damage at the corner is relatively serious. In addition, the stress distribution of the roadway floor is reduced. The increase of shear modulus has no obvious effect on the volume and range of plastic zone on both sides of the roadway. As shown in Figure 11, stress concentration also occurs at the bottom corner of roadway.

Figure 12 shows the displacement magnitude under the condition that the shear modulus is different. Based on Figure 12, it can be known that increasing the shear modulus has apparent influence on the displacement along the horizontal direction and the displacement along the vertical direction. When the shear modulus is small, it has relatively large impact on the displacement variation of the roadway. Along the direction of x-axis, the shear modulus gradually increases. When the shear modulus is small, the displacement of both sides of the roadway will have a significant impact. When the shear modulus continues to increase, the influence of the shear modulus on the horizontal displacement of the surrounding rock of the roadway will gradually decrease. Along the direction of the z-axis, with the increasing of the shear modulus, the deformation magnitude of the roadway roof decreases gradually.

Figure 13 shows the variation of the stress when the shear modulus is different. It can be seen from Figure 13 that the change of shear modulus has no significant effect on the stress distribution of surrounding rock of roadway. When the shear modulus increases, the stress tends to increase. This further indicates that the characters of the rock mass properties have certain influence on the distribution of the stress around the roadway.

5. Conclusions

In this paper, numerical simulation with the three-dimensional software FLAC3D was conducted to analyse the stress and displacement distribution around the rectangular roadway. The influence of kinds of parameters on the plastic zone, stress variation, and displacement variation of the roadway was studied. The numerical simulation results were compared with theoretical analysis. There was a close match between the numerical simulation results and the theoretical analysis results. This confirmed the effectiveness of the numerical simulation method. Based on this study, the main conclusions are summarized as follows:

(1) The deformation of both sides of rectangular roadway and roof will change with the change of surrounding rock properties. It is found that the roadway side and the roadway corners are the core position that needs to be especially supported during the roadway support

(2) The plastic zone range or volume of surrounding rock of rectangular roadway will change obviously with the change of surrounding rock strength. In addition to this, the increasing trend of the plastic zone at the roadway side and the roadway corners is larger than that of the roof. This further indicates that during the excavation process of the roadway, the roadway side and the roadway corners are the weakest part to be damaged

(3) When the strength of the surrounding rock mass increases, the ability that the surrounding rock mass around the roadway can bear the stress increases apparently

Data Availability

The data appearing in the manuscript is available by contacting the corresponding author after the publication of the manuscript.

Disclosure

This article is organized under the joint efforts of all the authors, and the authors have agreed on the order in which the papers should be signed.

Conflicts of Interest

The authors declare that they have no conflicts of interest.

Acknowledgments

The paper is supported by the State Key Laboratory Cultivation Base for Gas Geology and Gas Control (Henan Polytechnic University) (WS2021A03), the Fundamental Research Funds for the Central Universities (2022JCCXXNY06) from China University of Mining and Technology, Beijing, and the Open Fund of State Key Laboratory of Water Resource Protection and Utilization in Coal Mining (SHJT-17-42.16, 2020108, and SHGF-16-25QL).

References

[1] H. P. Xie, F. Gao, and Y. Ju, "Research and development of rock mechanics in deep ground engineering," *Chinese Journal of Rock Mechanics and Engineering*, vol. 34, no. 11, pp. 2161–2178, 2015.

[2] H. P. Xie, F. Gao, Y. Ju et al., "Quantitative definition and investigation of deep mining," *Journal of China Coal Society*, vol. 40, no. 1, pp. 1–10, 2015.

[3] Y. Xue, J. Liu, P. G. Ranjith, F. Gao, H. Xie, and J. Wang, "Changes in microstructure and mechanical properties of low-permeability coal induced by pulsating nitrogen fatigue fracturing tests," *Rock Mechanics and Rock Engineering*, vol. 55, no. 12, pp. 7469–7488, 2022.

[4] Y. Xue, P. G. Ranjith, Y. Chen, C. Cai, F. Gao, and X. Liu, "Nonlinear mechanical characteristics and damage constitutive model of coal under CO_2 adsorption during geological sequestration," *Fuel*, vol. 331, article 125690, 2023.

[5] W.-j. Wang, S.-q. Li, and G.-b. Ouyang, "Studay on technique and test of surrounding rock control of deep shaft coal roadway," *Chinese Journal of Rock Mechanics and Engineering*, vol. 10, pp. 2102–2107, 2006.

[6] W.-f. Li, "Numerical simulation analysis of large section rock roadway support based on FLAC3D," *Journal of China Coal Society*, vol. 27, no. 6, pp. 12–15, 2018.

[7] R.-l. Zhang, J.-c. Wang, and J.-m. Zhu, "Research on the supporting parameter optimization for the supporting top coal of the large section tunnel," *China Mining Magazine*, vol. 21, no. 12, pp. 96–99, 2012.

[8] R.-l. Shan, X.-s. Kong, B. Li, P. Shan, and Y. Xia, "Supporting design and optimization of large section roadway with straight wall and semicircle arch," *China Mining Magazine*, vol. 23, no. 1, pp. 87–91, 2014.

[9] J.-h. Chen, P. Liu, H.-b. Zhao, C. Zhang, and J.-w. Zhang, "Analytical studying the axial performance of fully encapsulated rock bolts," *Engineering Failure Analysis*, vol. 128, article 105580, 2021.

[10] M.-g. Qian and P.-w. Shi, *Mine Pressure and Strata Control*, China University of Mining and Technology Press, Xuzhou, China, 2010.

[11] Q.-b. Meng, L. Han, W.-g. Qiao, D.-g. Ling, and H. Li, "Numerical simulation research of bolt-grouting supporting mechanism in deep soft rock roadway," *Journal of Mining & Safety Engineering*, vol. 33, no. 1, pp. 27–34, 2016.

[12] M.-c. He, X.-y. Wang, W.-t. Liu, and S.-b. Yang, "Numerical simulation on asymmetric deformation of deep soft rock roadway in Kongzhuang Coal Mine," *Chinese Journal of Rock Mechanics and Engineering*, vol. 27, no. 4, pp. 673–678, 2008.

[13] X.-l. Jia, "Study on numerical simulation of surrounding rock stability of deep roadway based on FLAC3D," *China Energy and Environmental Protection*, vol. 39, no. 6, pp. 18–22, 2017.

[14] Y.-h. Shang, Q.-y. Shan, L.-k. Xie, and G. Guo, "Numerical simulation on deep laneway surrounding rock deformation based on FLAC3D," *Modern Mining*, vol. 27, no. 5, 2012.

[15] Z.-j. Su, S.-z. Du, H.-x. Huang, and Z.-b. Fan, "Numerical simulation analysis of deformation and damage of deep tunnel's surrounding rock," *The Chinese Journal of Geological Hazard and Control*, vol. 27, no. 2, pp. 121–126, 2016.

[16] X.-t. Zhang, "Study on surrounding rock stability of deep roadway support based on FLAC3D," *China Energy and Environmental Protection*, vol. 40, no. 1, 2018.

[17] J.-h. Chen, H.-b. Zhao, F.-l. He, J.-w. Zhang, and K.-m. Tao, "Studying the performance of fully encapsulated rock bolts with modified structural elements," *International Journal of Coal Science and Technology*, vol. 8, no. 1, pp. 64–76, 2021.

[18] Q.-y. He, L. Zhu, Y.-c. Li, D.-q. Li, and B.-y. Zhang, "Simulating hydraulic fracture re-orientation in heterogeneous rocks with an improved discrete element method," *Rock Mechanics and Rock Engineering*, vol. 54, no. 6, pp. 2859–2879, 2021.

[19] L. Mu and L.-g. Zhao, "Research on surrounding rock stability and supporting parameter design based on FLAC3D numerical simulation," *China Energy and Environmental Protection*, vol. 40, no. 12, pp. 170–173, 2018.

[20] R.-h. Zhou and D.-y. Wu, "Stress field and displacement field analysis of coal rocks based on FLAC 3D numerical simulation," *Journal of Lanzhou Institute of Technology*, vol. 24, no. 3, pp. 26–30, 2017.